Additive manufacturing of geopolymer for sustainable built environment

Biranchi Panda*, Suvash Chandra Paul, Lim Jian Hui, Yi Wei Daniel Tay, Ming Jen Tan

Singapore Centre for 3D Printing, School of Mechanical & Aerospace Engineering

Nanyang Technological University, 50 Nanyang Avenue, Singapore 639798

Abstract

This paper evaluates the potential of fly ash based geopolymer cement for large scale additive manufacturing (AM) of construction elements. Geopolymer is considered as a green construction material and its use in AM may contribute towards sustainable environment since in AM process material is only deposited whereby it is necessary. As part of this research, an industrial robot was employed to print geopolymer mortar in layer-by-layer manner directly from 3D computer-aided design (CAD) model. The characteristic of raw materials and fresh properties were examined by rheology, x-ray diffraction (XRD), and scanning electron microscopy (SEM). Mechanical tests such as compression, flexural and tensile bond strength were conducted on the printed geopolymer in different printing directions and their performance was compared with casted samples. It was found, from the experimental results, that the mechanical properties of 3D printed geopolymer are mostly dependent of loading directions due to anisotropic nature of the printing process and retains intrinsic performance of the material.

Keywords: Digital Construction, Geopolymer, Additive manufacturing and Sustainable environment

---

*Corresponding author Email: biranchipanda@tecnico.ulisboa.pt

1. Introduction

After more than 25 years of research and development, additive manufacturing (AM) is still continuing to grow in various industrial domains, such as aerospace, automobile and medical, with introduction of new technologies, methods and applications [1-3]. Out of all, building and construction (B&C) sector appears to be lagging in terms of technology and innovation unlike other manufacturing industries. Our current construction process continues to be relatively simple and systematic; requiring cumbersome formwork and much skilled labor to build any kind of freeform structures [4]. With evolution in time, the construction designs are becoming more complicated and the workers involved in this process are increasingly exposed to unhealthy environments [5]. This compels many researchers and industry experts to explore technologies like large scale additive manufacturing or 3D printing to bring automated solutions in the construction process.

3D concrete printing technology can be categorized in two major categories i.e. D-shape and contour crafting [6-9]. Both technologies have proven to be effective means of printing complex geometrical structures as part of rapid construction technique [10]. Though the printing processes in both technologies are similar in a sense that objects are directly made from the CAD models, actually they are developed for different applications and materials. In D-shape, sand and binder are used together to create stone-like free-form structures [9], where, sand is initially deposited over the build plate and then the binder is injected as per the digital model to hold the sand particles at that precise location. Once the printing is finished, excess sand is washed away from the built plate by a blowing air to the part geometry [11]. The major limitation of this method is that only limited materials can be allowed whereas, in contour crafting, a wide variety of materials can be

extruded out layer-by-layer to print a single house or a colony of houses, while imbedding conduits for electrical, plumbing and air-conditioning [3]. Soon after the development counter crafting, few researchers and industries have successfully printed and characterized various cementitious material using Ordinary Portland Cement (OPC) as a key binder in their mix compositions [12-18]. To reduce global warming effect due to OPC, some authors also tried to replace the cement with some industrial by-products such as fly ash and slag that are collected from different power plant industries. However, 100% replacement of cement or development of new environmental friendly material have never been an easy task. In this regard, recently, Xia et al. [19] presented a new methodology of formulating geopolymer material for powder-based 3D printers. As discussed before, powder-based printing is highly suitable for small-scale building components which limits the technology for large scale construction. Therefore, this research aims to develop an extrusion based fly ash geopolymer for large scale concrete printing application. Geopolymer is considered as a green construction material since its main ingredients such as fly ash and slag are collected from industrial wastes. It is synthesized by the reaction of aluminosilicate materials with user friendly alkaline reagents i.e sodium or potassium silicates [20-22]. Successful application of fly ash based geopolymer is believed to reduce our dependency on the OPC.

The main goal of this paper is to develop 3D printable geopolymer material that have never done before for extrusion based large scale printing system. No-slump, extrudable geopolymer was formulated by performing preliminary investigation described in section 2. Later, mechanical properties of printed samples were investigated and compared with conventionally casted (in-situ) geopolymer to reveal anisotropy behavior resulting from the extrusion process. In addition, microstructure analysis was carried out to support the geopolymer reaction and final product.

2. Preliminary Investigations

Prior to experiments presented in the third part of this paper, a preliminary investigation was conducted to verify the thixotropic behavior of the concrete, i.e material supposed to have high yield stress at the beginning (rest period) and become less viscous when agitated or stressed, but again rebuilds or re-flocculates to initial state once comes to rest [23]. Unlike conventional casting, 3D concrete printing process requires a continuous, high degree control of material during printing where traditional concrete cannot be used directly. Shape retention and extrudable are two contradicting characteristics that need be to be fulfilled while developing new materials for concrete printing application.

In this investigation, a typical fly ash based geopolymer was formulated using potassium silicate as alkaline reagent. The mix proportion was then manipulated by changing the type and amount of admixtures and/or additives (like actigel, nano clay) to achieve shape stability. For buildability, we used our custom-made plate stacking test (Figure 1) to monitor the deformation upon subsequent loading of the layers. Material having high yield stress was found to show less deformation on loading and to achieve this property we optimize the packing density by grading different raw materials in Microtrac S3500 Particle Size Analyzer. However, due to high yield stress, the material was not extrudable through a 25-mm diameter hose pipe. Then referring to an article by Choi et al. [24], we adjusted the paste volume to enable a lubrication layer that helped us for smooth flowing of geopolymer inside the hose. Note that, due to stick nature of alkaline reagent the pressure during extrusion was fluctuating between 10-15 bar, i.e 75 part of maximum allowable pressure as mentioned by the pump manufacture.

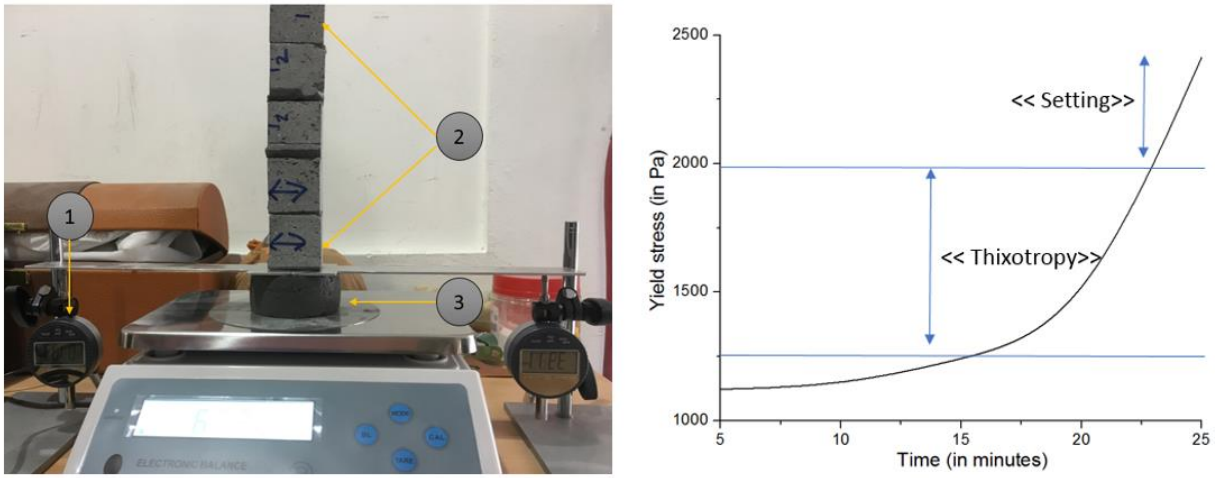

Figure 1. (a) Green strength characterization using plate stacking test (1. Dial gauge 2. Added weights 3. Fresh geopolymer) (b) Early age property obtained from Rheometer

Based on trial-and-error, we obtained a geopolymer mixture that can be extrudable and retain its shape after printing. From the experimental trails, a stress range (figure 1(b)) was also identified, within which the custom made geopolymer was suitable for 3D printing application. More details of the used materials and experiments are described in the later sections of this paper.

3. Materials and Methods

3.1 Collection of raw materials

The commercially available CEMGUARD® fly ash in India was used as key binder in this research. Figure 2 shows the typical morphology (spherical in shape) of the as-received fly ash. It is classified as class F according to ASTM C618-12a, ($SiO_2 + Al_2O_3 + Fe_2O_3 = 89.15\% > 70\%$ and $CaO < 10\%$) [25]. Ground granulated blast-furnace slag (GGBS) and micro silica (silica fume) were provided by Engro and Elkem Pvt Ltd Singapore respectively. The chemical compositions of both fly ash and GGBS are presented in table 1. Due to restrictions of nozzle diameter, we have used river sand as fine aggregates in this research. The particle size distribution of all the raw materials are plotted in figure 3.

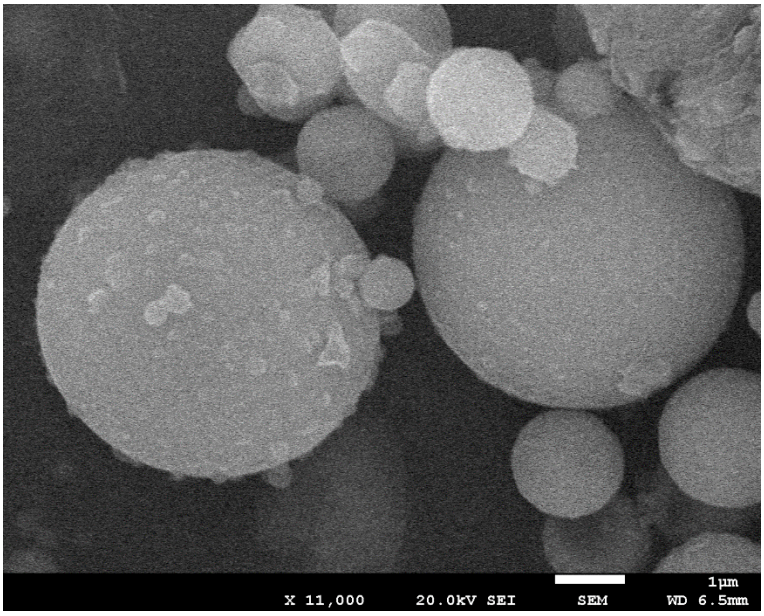

Figure 2. Scanning electron microscope (SEM) micrographs of fly ash

Table 1 The chemical composition of Fly ash and GGBS

	SiO_2	Al_2O_3	Fe_2O_3	CaO	MgO	TiO_2	K_2O	SO_3
Fly ash	58.59	30.44	4.66	1.21	0.776	2.02	1.51	0.09
GGBS	30-40	7-17	0.1-1.8	30-50	2-14	NA	NA	NA

For the geopolymerization, potassium hydroxide and potassium silicate solutions were used as the alkaline reagent. Potassium silicate (SiO_2 =24.94%, K_2O=19.09%and water=55.97%) was obtained from Noble Alchem Pvt. Ltd, India whereas potassium hydroxide is prepared in the lab by dissolving pallets in distilled water to obtain 8M molarity. Both potassium hydroxide and potassium silicate were mixed together to obtain 1.8 molar ratio and stored at room temperature of 25±2 ◦C for 24 h before using them in geopolymer mix.

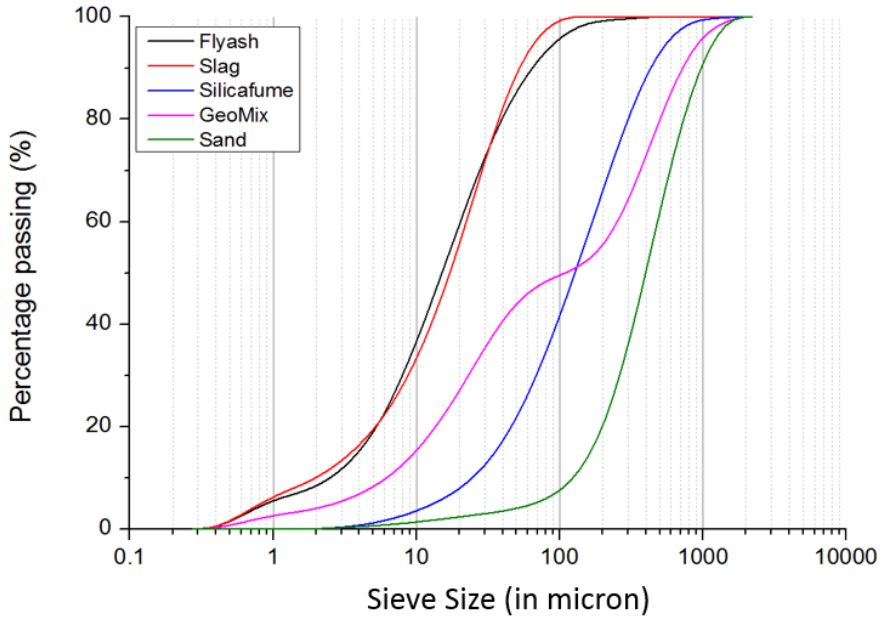

Figure 3. Particle size distributions obtained from Mastersizer 2000

3.2 Synthesis of geopolymer

All the dry materials, i.e., fly ash, GGBS and silica fume were blended together (as per Table 2) in a Hobart planetary mixer (slow speed) for 2 to 3 minutes followed by addition of thixotropic additives (Actigel and cellulose) to achieve no-slump extrudable geopolymer. Then the dry mix was activated by adding alkaline solution (potassium silicate) for around one minute in medium speed. Soon after, fine river sand was poured and mixed homogenously for another 1-2 minutes. At the end, slight addition of water was allowed for getting good workability of the mix. Now the geopolymer is ready for both casting and printing. It is important to note that the properties of geopolymer mortar may change after being extruded out from the hose pipe depending on the pump pressure, length of hose pipe, geometry of the nozzle, etc.

Table 2. Mix design of 3D printable geopolymer mortar

Materials	Weight by Percentage
Fly ash	27.85
Slag (GGBS)	1.68
Silica Fume	3.36
Thixotropic filler	0.875
Sand	49.55
Potassium Silicate	12.5
Water	4.16

3.3 Casting and printing of geopolymer

All the casted and printed samples were prepared from one batch of geopolymer mix and the respective tests were tested after 28days of ambient curing. For printing, a 15/7 (length/width) mm rectangular nozzle was used to deposit geopolymer layer by layer, controlled by 3D CAD/CAM program (see figure 4). The print path was first generated from the 3D model of the desired object, using 3D-2D slicing software, which slices the 3D shape of the object into layers of constant thickness. A six axis Denso ® robot, mounted on a holonomic platform, printed 500×300×85 mm rectangular slab while depositing geopolymer mortar at a speed of 120mm/sec. During the entire printing process, hose pipe length (3 meter) and pump flow rate (3 L/min) were kept constant to avoid any inadvertent effect on print quality. Figure 5 shows the overview of our printing process starting from modelling to layer-by-layer deposition. After the printing, 50 mm cubes and 40 x 40 x 160 mm prisms were taken out from the slab in different directions (by sawing) to carry out a comparative mechanical test of the casted samples. For casting, similar dimensions of cube (50 mm) and prism (40 x 40 x 160 mm) were used and cured simultaneously with the printed samples.

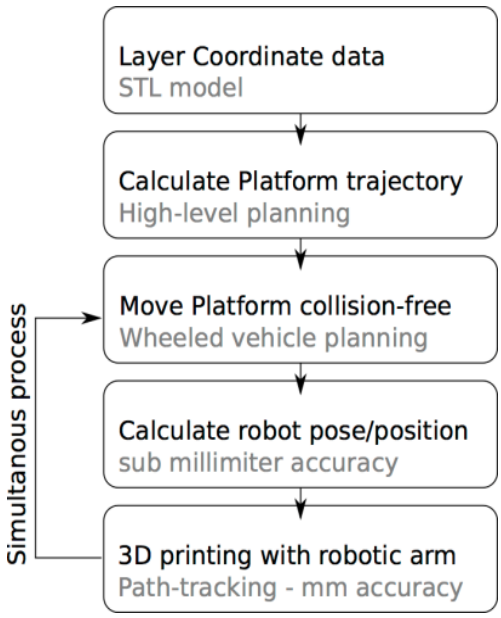

Figure 4. 3D concrete printing process pipeline

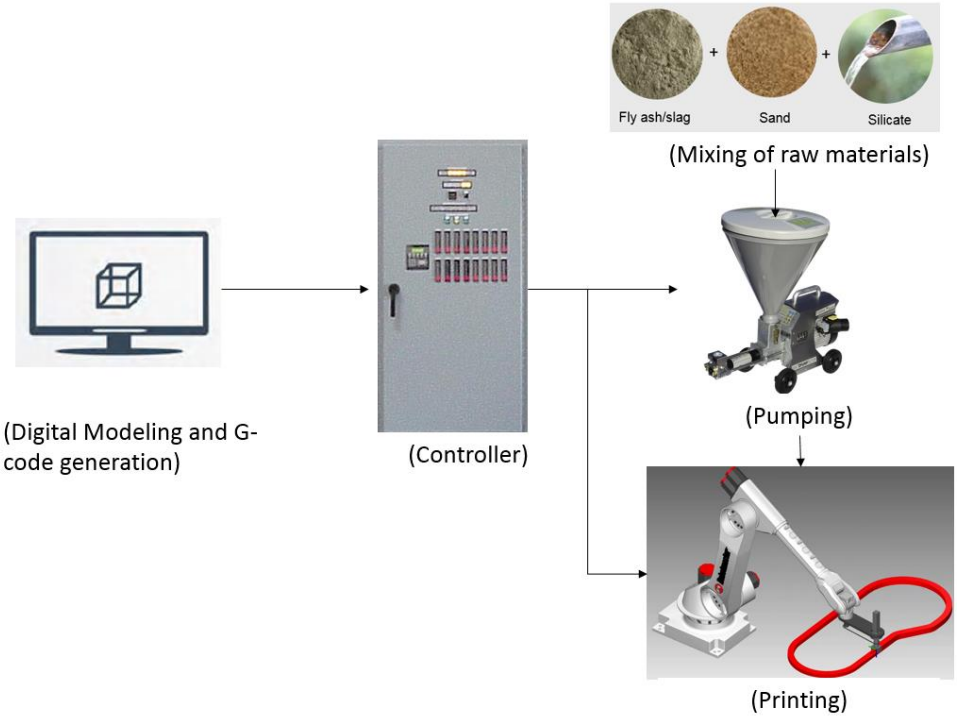

Figure 5. Schematic of the 3D concrete printing setup

3.4 Experimental procedures

3.4.1 Rheology of printable geopolymer

The fresh properties especially rheology of geopolymer, including yield stress and plastic viscosity are very important for concrete printing since the print quality as well as the hardened properties are directly related to its fresh properties. Yield stress corresponds to the shear stress required to initiate the flow of fresh concrete, whereas the plastic viscosity measures the resistance to flow after flow is initiated [26]. In this research, Viskomat XL from Schleibinger testing systems, Germany was used to study the rheology of geopolymer mortar. The Viskomat XL consists of a three-liter container with one rotating four blade vane (diameter 69 mm, height 69 mm) inside it. After the material is loaded in to this container, flow curve test was performed at increasing speed of 60 rpm up to two minutes followed by two-minutes constant speed and then reducing to zero in two minutes. The area of T (Torque) - N (rotation, rpm) graph was used to measure thixotropic index whereas the down curve is considered to calculate Bingham parameters of the mortar i.e. plastic viscosity, and shear stress [27].

3.4.2 Density

The bulk densities of casted samples were measured by taking average from three samples after 28 days of ambient curing. For printed part, 50 mm cubes (extracted from 500×300×85 mm slab) were considered for density measurement similar to the mould-casted samples.

3.4.3 Compression, tensile (bond) and flexural test

Compressive strengths were measured for both casted and printed samples using ALPHA 3-2000A model tester at a loading rate 100KN/min. All the samples were mostly 50 mm cubes. For printed elements, total twenty-seven cube samples were extracted from 500×300×85 mm slab and tested in compression for 7, 14 and 28 days (nine samples each day). The samples were loaded in three

different directions as shown in figure 6 and their average values are noted considering three samples in each direction.

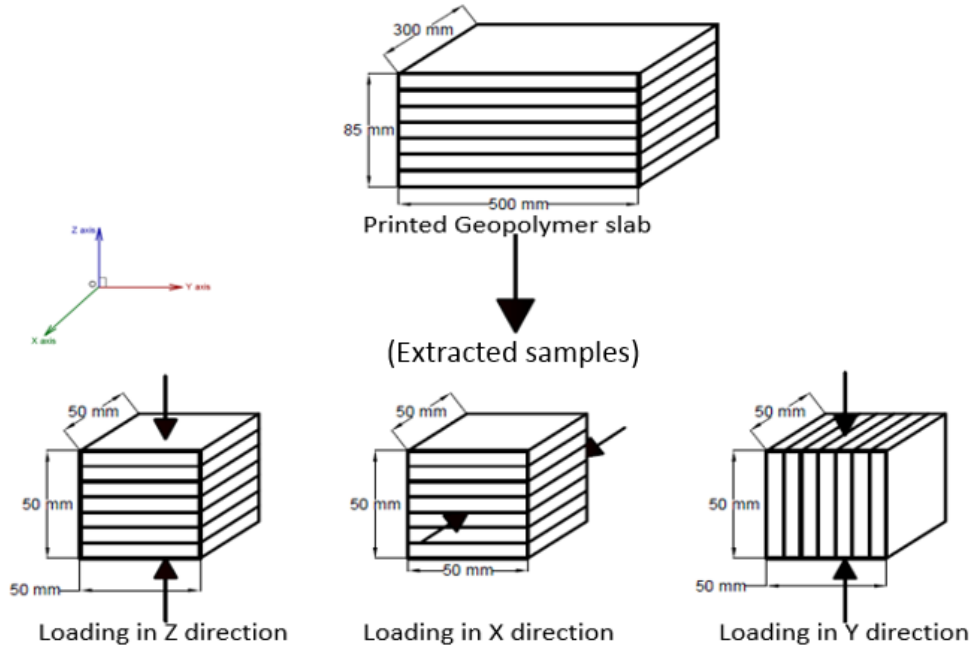

Figure 6. The testing directions for mechanical properties

Like compression test, 40 x 40 x 160 mm prisms were extracted from the printed slab and tested in three directions using Instron 5960 dual column system at a loading rate of 10 N/sec. In total 18 prisms (12 printed and 6 casted) are tested at the age of 7 and 28 days under 3-point bending load and their averages values were reported. It is important to note that the mechanical strengths of printed samples are mostly dependent on the time gap between the layers which is further linked to size of the sample and printing speed. Therefore, we additionally conducted tensile bond strength of printed geopolymer by varying the time gap from five to twenty minutes. Two layers were printed with different time gaps (5,10,15 and 20 mins) and later a section (50x15) is extracted from it for performing the bond test by adhering the free surface to the jig with a rapid hardening glue.

3.4.4 Microstructure characterization

X-ray diffraction (XRD) and field emission electron microscopy (Fe-SEM) were used to characterize the raw materials and phase changed during poly-condensation process in geopolymer [28]. For this purpose, randomly oriented powder sample (about 1 g in weight) was prepared (for XRD) by grinding dried portions of the tested samples and respective scan patterns were obtained for 2theta values between 10 to 80 degree using Pan Analytical Empyrean with CuKa source at room temperature. To see the microstructure and interfacial transition zone (ITZ), 25 mm diameter sample was prepared from the geopolymer cube at the age of 28 days following sectioning-grinding-polishing activities. Due to non-conductive properties, samples were coated using a gold sputter coater prior to imaging to ensure that there is no arching or image instability during micrograph collection. Fe-SEM analyses were performed using a JEOL JSM-7600F microscope equipped with an energy dispersive X-ray analyzer.

4 Results and Discussion

4.1 Rheology

Figure 7 shows the torque-speed (T-N) graph of geopolymer mortar obtained from the rheometer with 10 minutes' time gap interval. From the classification of non-newtonian fluids, it was concluded that the material behavior is thixotropic in nature that can be defined by reversible, isothermal, time-dependent decrease in viscosity when a material is subjected to increased shear stress or shear rate [29]. Thixotropy property has a critical role for concrete printing application. Due to high yield stress and low viscosity material can easily extrudable without losing its stability.

Quantitative measurement of thixotropy, obtained from the area held between up and down curve of T-N graph, reveals the minimum thixotropy value for the current geopolymer mix should be 10,000. However, this value depends on test set up, mix design and shear rate applied by

rheometer. The decrease of thixotropy over time (below figure) indicates our material open time i.e the time in which the fresh concrete is reasonably extrudable. Below the minimum value of thixotropy, material is not suitable for large scale printing application.

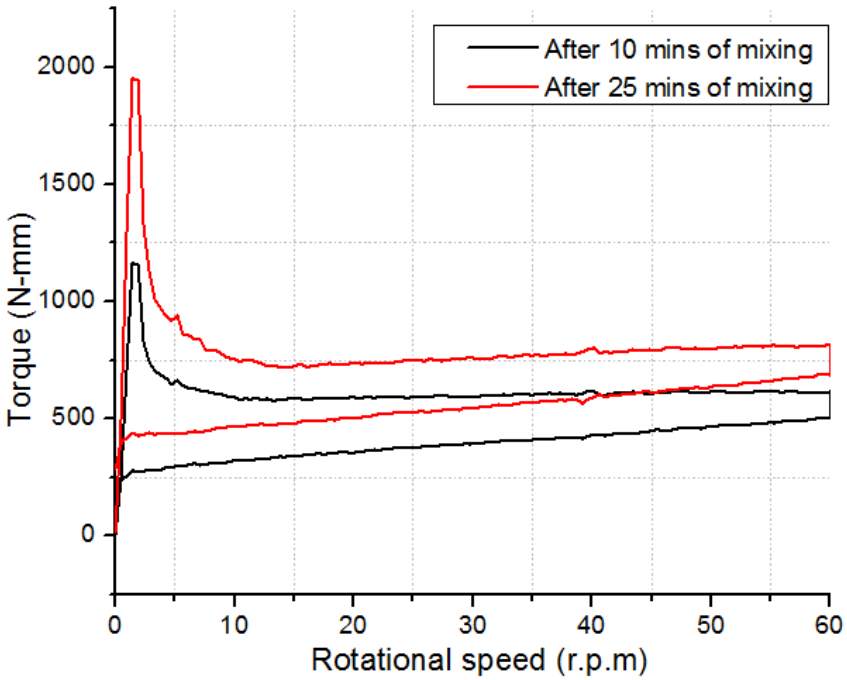

Figure 7. Geopolymer rheology with time

4.2 Density

The average density of casted specimen was found to be 2150 kg/m^3 whilst that of printed specimen was a little higher at 2250 kg/m^3. This is most likely due to minimal yet forceful pressure exerted by the pump during extrusion. Various printing samples were iterated with the goal of progressively improving their quality by aiming towards a more compact final product. This comparison is shown in Figure 8.

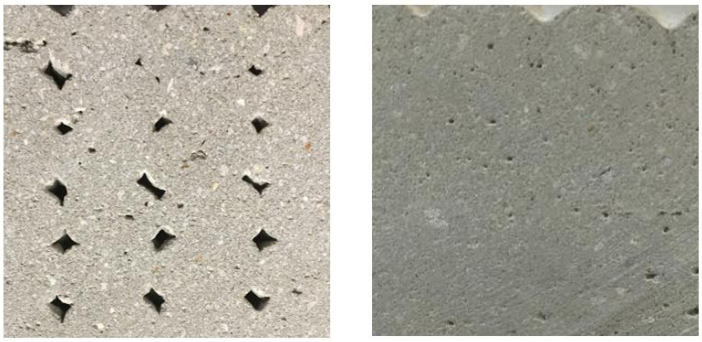

Figure 8. Cross section view of two different printing processes

4.3 Compression, tensile (bond) and flexural test

Figure 9 (a) shows compressive strengths of casted as well as printed samples after 7, 14 and 28 days of preparations. From the test results, it was found that printed geopolymer samples are stronger in the Y loading direction compare to X and Z directions. This behavior can be well explained by mimicking micro-mechanics of composite material where it has been seen that for loading in a plane perpendicular to layers allow direct transfer and distribution of load uniformly throughout the cross-section but in case of loading in transverse direction, the beads start to slip/separating from each other causing lower strength in specimen. Comparing the performance with casting, the printed samples were found to be ≃5% weaker in the X and Z directions while ≃2% stronger in Y direction. A pioneer research group from Loughborough University, UK has confirmed the importance of these variations occurring in the 3D printed samples [12].

Figure 10 shows the variations in bond strength measurement with respect to different printing time gap resulted in geopolymer samples. It is evident from the decreasing pattern that a delay in layer deposition causes lower strength in the part due to poor bonding between interfacial layer surfaces. As the material get hardened with past of time, the layer adhesion property goes on

decreasing, thus low mechanical properties are obtained if material is not properly designed considering the part geometry.

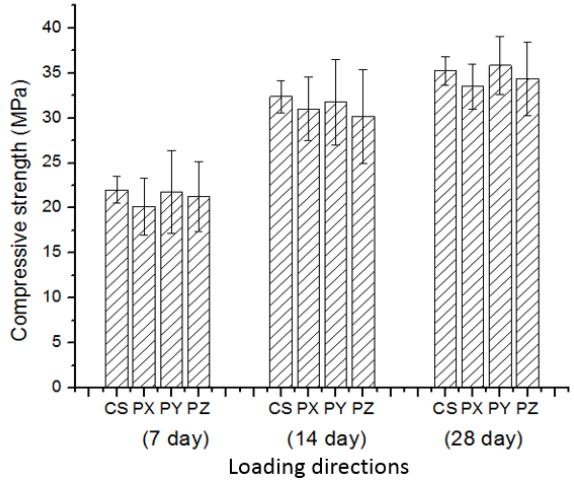

(a)

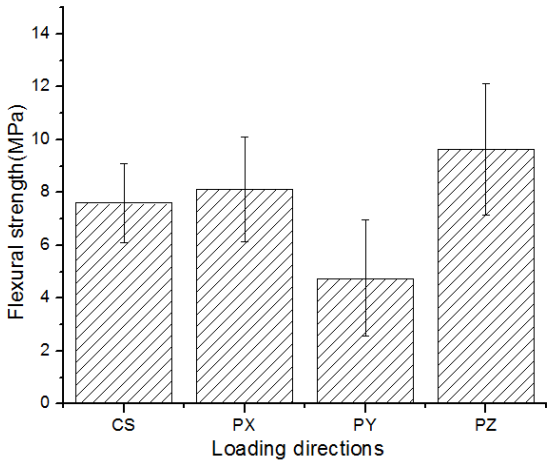

(b)

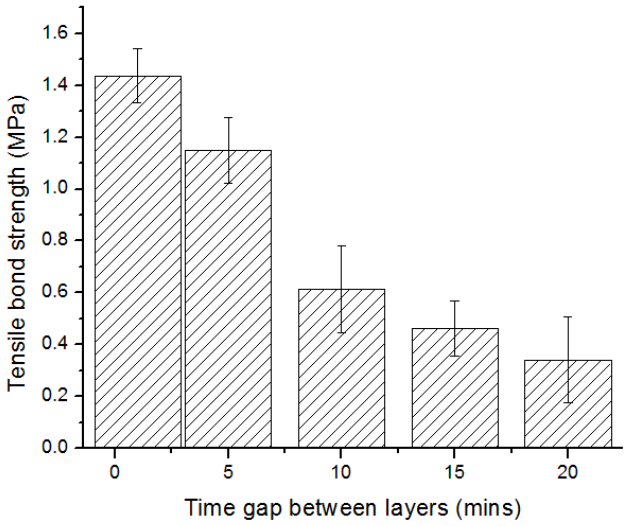

(c)

Figure 9. Variation of (a) compression (b) flexural-28 days (c) tensile bond strength-28 days (with time gap) of printed geopolymer compared to standard casted samples where CS: Casted sample; PX, PY and PZ: printed sample loading in X, Y and Z direction (refer figure 6)

Similar to the compressive strength, flexural strength of printed geopolymer was also dependent upon loading directions due to anisotropy of the 3DP process. All the printed geopolymers were loaded in X, Y and Z directions (refer Fig. 6) for 3-point bending test after 28 days of printing. Compared to casted samples, the printed specimen exhibited higher flexural strength in "X" and "Z" directions (Figure 9 (c)) due to well compaction of the central area, where maximum tensile stress used to occur during loading. However, "Y" direction was found to be offer lowest flexural stress because of tensile force acting perpendicular to the layer direction. To improve this direction strength, addition of reinforcement can be considered in future which may improve the bonding between the layers. Moreover, advance research in terms of modeling and simulations are needed to confirm the findings of experimental outcomes.

4.4 Microstructure Characterization

The XRD patterns of fly ash and geopolymer are presented in figure 10. Quartz and mullite are the major crystalline phases of the fly-ash which are unreactive in the geopolymeric reaction, and act as filler [30]. Nevertheless, the amorphous aluminosilicate broad hump produced between 2 theta = "20 and 30" characterizes the reactive and dissolvable content in alkaline solution during the geopolymer development. The amorphous phase was recognized as one of the most important factors that influence the physical and mechanical properties of fly ash geopolymers: the higher the amount of amorphous phase, the greater the strength exhibited by the geopolymer. Comparing XRD patterns of fly ash, the intensity of crystalline peak at 2 theta angle of 17, 35, and 40 degrees was found to be much less in the geopolymer, which is a clear indication of geopolymerization. This behavior is completely in agreement with a recent research conducted by Khan et al [31] for ambient curing low Ca fly ash based geopolymer.

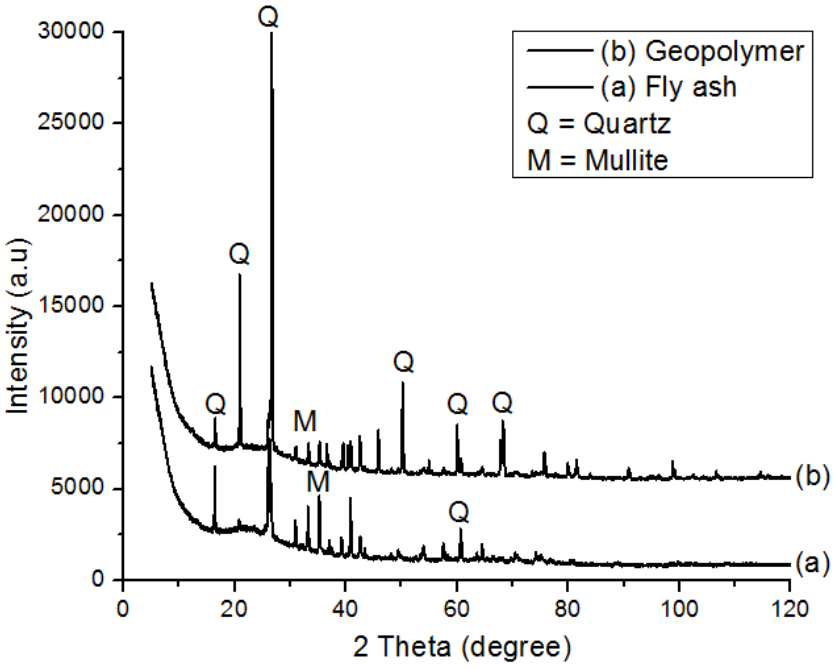

Figure 10. XRD patterns of Fly ash and Geopolymer

The Fe-SEM micrographs of casted geopolymer is shown in figure 11. It is obvious that the incorporation of different additives in geopolymer composites has significantly influenced the formation of binding gels and ultimately the hardened microstructure. Majority of fly ash particles have dissolved during alkalination with little traces of unreacted or partially reacted fly ash particles. However, interfacial transition zone (ITZ) revealed (figure 11(b)) the presence of some micro pores, that might have reduced compressive strength of the geopolymer. More research can be done in this direction to improve the ITZ by fully characterization the microstructure since it plays a critical role in mechanical, transfer properties and consequently the long-term performance of concrete [32].

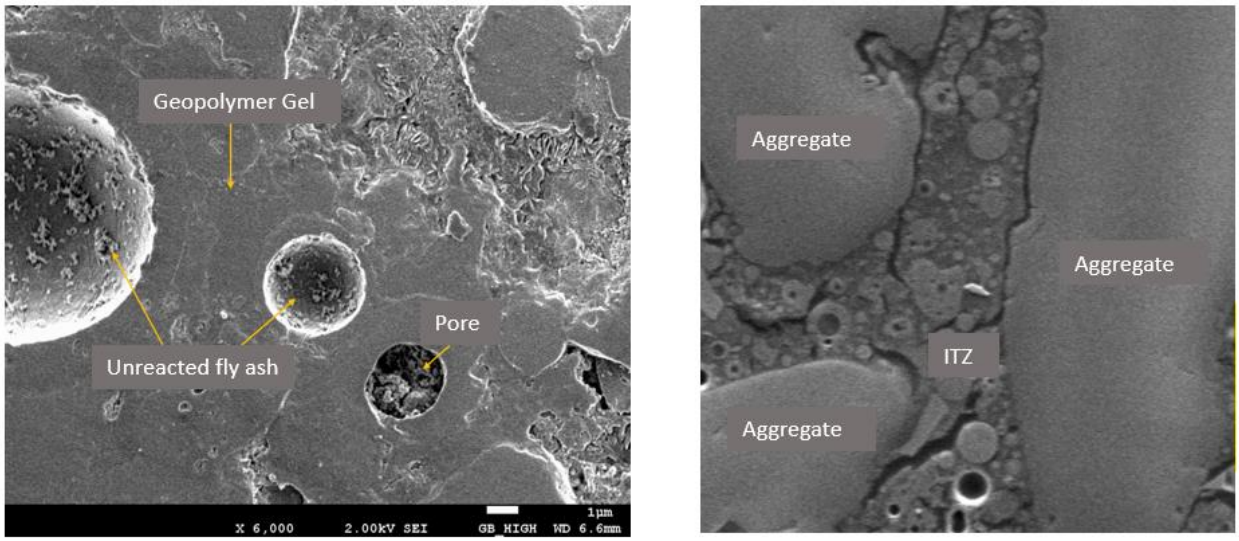

(a) (b)

Figure 11. (a) SEM micrograph (b) Interfacial transition zone (ITZ) of fly ash geopolymer

5 Concrete printing research and its limitations

Additive manufacturing of concrete is being explored in many places around the world. The focus is mainly on a trial-and-error based exploration of the possibilities. However, to obtain a viable manufacturing technology and realize the potential, a higher level of process control is required. Figure 12(b) shows some concrete printed parts that are designed and printed at Nanyang Technological University (NTU), Singapore with the help of Denso® robot and 4 axis gantry system while co-relating the material, machine and structure of the final part (figure 12(a)). From the author's own experience, it is always suggested to understand the material fresh properties and printer capabilities before designing part for AM of concrete, so that based on the requirements, materials and print path can be adjusted to incorporate complexity present in the freeform design [33,34].

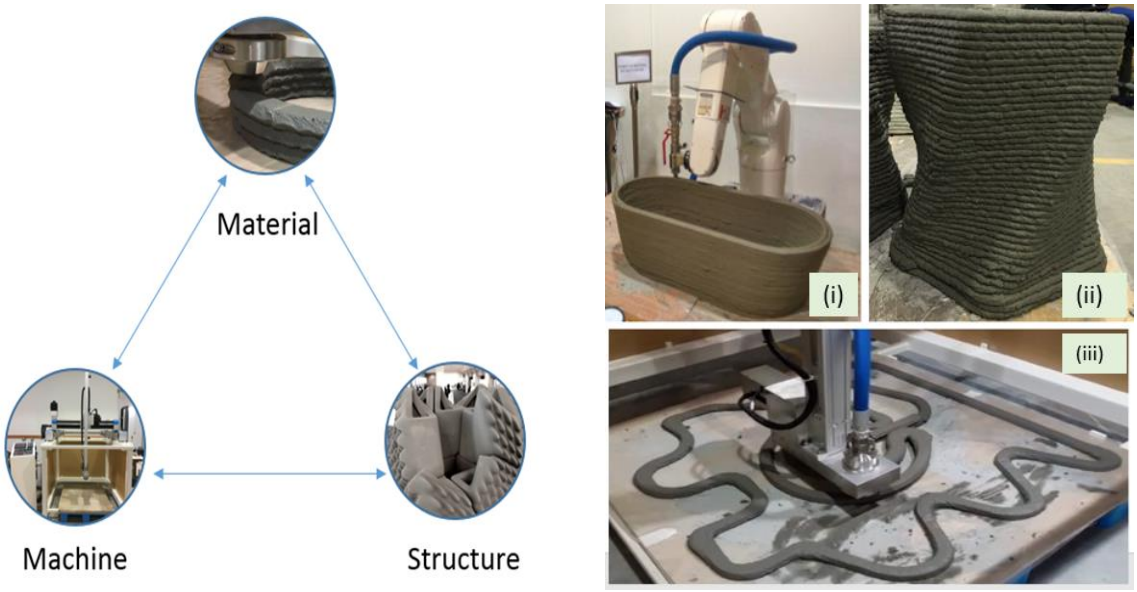

Figure 12. (a) 3D Concrete printing components (b) robot assisted concrete printed (i) bath tub (ii) helix tower and (iii) freeform design by large scale gantry

Notwithstanding the exciting projects are running around the world, introduction of concrete printing in load bearing structures is still some distance away. Some issues are necessarily to be solved in this regard. These are:

Reinforcement placement: For structural safety and reliability, reinforcements are needed in concrete printed parts. Few years back, an initiative was taken by Chinese company, Winsun by adding reinforcement manually in to concrete printed form work [35]. However, till now it is not clear to what extent those structures are applied structurally, and what strategies have been applied to achieve structural safety. Alternatively, for the first time, researchers at TU/e demonstrated the ability to print concrete in combination with steel reinforcement and fiber [36, 37]. Significant post-cracking deformations and post-cracking strength is achieved by printing reinforcement with concrete. Their future research will now aim at characterizing the cable behavior, optimizing the reinforcement placement for some structural elements.

Printing overhanging structures: Printing overhanging structures such as arch, dome, etc., is another common problem in concrete printing domain. In this case, support material can be used to handle this issue. Also, materials with rapid hardening behavior can solve this issue in some extent. The advantages of rapid hardening material (or set-on demand) is that it allows to print freeform structures with an angle of inclination, however the bond between the layers will not be strong enough for structural loading situations. Therefore, enough care should be taken while designing the material for such kind of applications.

Multi-material printing: The real benefit of concrete printing lies in depositing different materials as per the need of applications. In order to happen this, the structure must be optimized based on loading conditions and then a multi head printed can simultaneously deposit materials like light weight, self-cleaning, self-healing as per the digital program fed in to the machine. This approach will bring a radically new and exciting way to our building designs.

Standard developments: Currently there is no guidelines available for 3D printing of construction materials. Therefore, for acceptance and use of printed parts in building and construction sectors, standards for materials, manufacturing process and structural design are highly necessary [38].

6 Conclusion

Extrusion-based 3D printable geopolymer mortar was developed in this study for the demand and lack of commercially available green construction material for large scale construction projects. Printed samples were subjected to mechanical strength testing in different directions and their performance was compared with standard casted geopolymer. The mould-cast geopolymer was found to exhibit higher compressive strength in "X" and "Z" direction with density of 2150 kg/m^3. The printing process increased the density up to 2250 kg/m^3, although, the layering process introduced small voids in the interstices between the extruded layers. In this regard, proper

selection of nozzle and slightly high pump pressure can be helpful in reducing the voids. The mechanical properties of 3D printed geopolymer were inevitably affected by the printing directions. Comparing to casted, printed sample exhibited higher compressive strength when load was applied in a plane perpendicular to the layers (i. e "Y"), however, in case of flexural sample, loading in the same direction resulted lowest strength followed by other two directions. This reduction can be attributed to the tensile force acting in between the layers which is weakest when compared when it acts along the layers (see graphical abstract). Like compression and flexural, tensile bond strength is also one of the critical parameter in concrete printing which was highly affected by time gap between layers and material open time. With increase in printing time gap, bond strength was found be decreased for the samples taken from same batch of material. Having said that, it is very important to balance material property like in case of spray painting where sufficient time is allowed for adhesion and self-support.

Additive manufacturing of geopolymer was introduced here as a promising technology to address the sustainable challenges in today's construction industry and open up new opportunities of design possibilities. However, the need to abolish conventional methods completely may not be necessary. The future of construction is most likely to be an integrated process that allows organizations to take advantage of both conventional and additive manufacturing technologies at the same time [39]. Considering the current importance digital construction, it is believed that 3D printing of geopolymer could be a breakthrough for faster and sustainable built environment. The outcomes of this research can be helpful to our future structural engineers for consideration of directional properties while designing a part for concrete printing application.

Acknowledgement

The research reported here has been supported by National Research Foundation Singapore (NRF) and Sembcorp Design & Construction Pte Ltd. The authors would like to acknowledge Catherine Soderberg (former graduate student of Harvard University's School of Design) for proofreading the article and improving its grammatical content.

References

[1] Chua, C. K., Leong, K. F., 2014. 3D printing and additive manufacturing: Principles and Applications (with Companion Media Pack) of Rapid Prototyping. World Scientific Publishing Co Inc.

[2] Gibson, I., Rosen, D. W., & Stucker, B., 2009. Additive manufacturing technologies: rapid prototyping to direct digital manufacturing. Springer Publishing Company, Incorporated.

[3] B. Khoshnevis, 2004. Automated construction by contour crafting - Related robotics and information technologies. Automation in Construction. 13(1), 5–19,

[4] Khoshnevis, B., Hwang, D., Yao, K. T.,Yeh, Z. 2006. Mega-scale fabrication by contour crafting. International Journal of Industrial and Systems Engineering. 1(3), 301-320.

[5] N. K. Kittusamy and B. Buchholz, 2004. Whole-body vibration and postural stress among operators of construction equipment: A literature review. J. Safety Res., 35(3), 255–261.

[6] Wu, P., Wang, J., Wang, X. 2016. A critical review of the use of 3-D printing in the construction industry. Automation in Construction, 68, 21-31.

[7] Kreiger, M. A., MacAllister, B. A., Wilhoit, J. M., & Case, M. P. 2015. The current state of 3D printing for use in construction. In The Proceedings of the 2015 Conference on Autonomous and Robotic Construction of Infrastructure. Ames. Iowa (pp. 149-158).

[8] Labonnote, N., Rønnquist, A., Manum, B., & Rüther, P. 2016. Additive construction: State-of-the-art, challenges and opportunities. Automation in Construction, 72, 347-366.

[9] D Shape: www.d-shape.com. (accessed on 5th July 2017).

[10] Lim, S., Buswell, R. A., Le, T. T., Austin, S. A., Gibb, A. G., & Thorpe, T. 2012. Developments in construction-scale additive manufacturing processes. Automation in

construction. 21, 262-268.

[11] Tibaut, A., Rebolj, D., Perc, M. N. 2016. Interoperability requirements for automated manufacturing systems in construction. Journal of Intelligent Manufacturing. 27(1), 251.

[12] Le, T. T., Austin, S. A., Lim, S., Buswell, R. A., Law, R., Gibb, A. G.,Thorpe, T. 2012. Hardened properties of high-performance printing concrete. Cement and Concrete Research. 42(3), 558-566.

[13] Le, T. T., Austin, S. A., Lim, S., Buswell, R. A., Gibb, A. G., Thorpe, T. 2012. Mix design and fresh properties for high-performance printing concrete. Materials and structures. 45(8), 1221-1232.

[14] Feng, P., Meng, X., Chen, J. F.,Ye, L. 2015. Mechanical properties of structures 3D printed with cementitious powders. Construction and Building Materials. 93, 486-497.

[15] Rushing, T. S., Rushing, T. S., Al-Chaar, G., Al-Chaar, G., Eick, B. A., Eick, B. A., Barna, L. 2017. Investigation of concrete mixtures for additive construction. Rapid Prototyping Journal. 23(1), 74-80.

[16] Perrot, A., Rangeard, D., Pierre, A. 2016. Structural built-up of cement-based materials used for 3D-printing extrusion techniques. Materials and Structures. 49(4), 1213.

[17] Hambach, M., Volkmer, D. 2017. Properties of 3D-printed fiber-reinforced Portland cement paste. Cement and Concrete Composites. 79, 62-70.

[18] Kazemian, A., Yuan, X., Cochran, E., Khoshnevis, B. 2017. Cementitious materials for construction-scale 3D printing: Laboratory testing of fresh printing mixture. Construction and Building Materials, 145, 639-647.

[19] Xia, M., & Sanjayan, J. 2016. Method of formulating geopolymer for 3D printing for construction applications. Materials & Design. 110, 382-390.

[20] Habert, G., De Lacaillerie, J. D. E., & Roussel, N. 2011. An environmental evaluation of geopolymer based concrete production: reviewing current research trends. Journal of cleaner productio. 19(11), 1229-1238.

[21] Davidovits, J. 1991. Geopolymers: inorganic polymeric new materials. Journal of Thermal Analysis and calorimetry. 37(8), 1633-1656.

[22] Nazari, A., & Sanjayan, J. G. 2015. Synthesis of geopolymer from industrial wastes. Journal

of Cleaner Production. 99, 297-304.

[23] Wallevik, J. E. 2009. Rheological properties of cement paste: thixotropic behavior and structural breakdown. Cement and Concrete Research, 39(1), 14-29.

[24] Choi, M., Park, K., & Oh, T. 2016. Viscoelastic properties of fresh cement paste to study the flow behavior. International Journal of Concrete Structures and Materials. 10(3), 65-74.

[25] ASTM C618-15, Standard Specification for Coal Fly Ash and Raw or Calcined Natural Pozzolan for Use in Concrete, ASTM International, West Conshohocken, PA, 2015.

[26] Banfill, P. F. 1991. The rheology of fresh mortar. Magazine of concrete research. 43(154), 13-21.

[27] Ahari, R. S., Erdem, T. K., Ramyar, K. 2015. Thixotropy and structural breakdown properties of self consolidating concrete containing various supplementary cementitious materials. Cement and Concrete Composites. 59, 26-37.

[28] Franchin, G., Scanferla, P., Zeffiro, L., Elsayed, H., Baliello, A., Giacomello, G., Colombo, P. 2017. Direct ink writing of geopolymeric inks. Journal of the European Ceramic Society. 37(6), 2481-2489.

[29] Kovler, K., Roussel, N. 2011. Properties of fresh and hardened concrete. Cement and Concrete Research. 41(7), 775-792.

[30] Provis, J. L., Van Deventer, J. S. 2007. Geopolymerisation kinetics. 1. In situ energy-dispersive X-ray diffractometry. Chemical engineering science. 62(9), 2309-2317.

[31] Khan, M. Z. N., Hao, Y., Hao, H. 2016. Synthesis of high strength ambient cured geopolymer composite by using low calcium fly ash. Construction and Building Materials. 125, 809-820.

[32] Demie, S., Nuruddin, M. F., Shafiq, N. 2013. Effects of micro-structure characteristics of interfacial transition zone on the compressive strength of self-compacting geopolymer concrete. Construction and Building Materials. 41, 91-98.

[33] Tay, Y. W. D., Panda, B., Paul, S. C., Mohamed, N. A. N., Tan, M. J., Leong, K. F. 2017. 3D printing trends in building and construction industry: a review. Virtual and Physical Prototyping, 1-16.

[34] Tay, Y. W., Panda, B., Paul, S. C., Tan, M. J., Qian, S. Z., Leong, K. F., Chua, C. K. 2016. Processing and properties of construction materials for 3D printing. In Materials Science Forum,

Trans Tech Publications.861, 177-181.

[35] Winsun: 3dprint.com, 2016b. Available from: https://3dprint.com/138664/huashang-tengda-3d-print-house/ [Accessed June 2017].

[36] Bos, F. P., Ahmed, Z. Y., Wolfs, R. J., Salet, T. A. 2018. 3D Printing Concrete with Reinforcement. In High Tech Concrete: Where Technology and Engineering Meet Springer, Cham. pp. 2484-2493.

[37] Salet, T. A., Bos, F. P., Ahmed, Z. Y., Wolfs, R. J., Ahmed Zeeshan Y. 2018. 3D Concrete Printing – A Structural Engineering Perspective. In High Tech Concrete: Where Technology and Engineering Meet. Springer, Cham. pp. X1iii- X1vii.

[38] Bos, F., Wolfs, R., Ahmed, Z., Salet, T. 2016. Additive manufacturing of concrete in construction: potentials and challenges of 3D concrete printing. Virtual and Physical Prototyping. 11(3), 209-225.

[39] Gosselin, C., Duballet, R., Roux, P., Gaudillière, N., Dirrenberger, J., Morel, P. 2016. Large-scale 3D printing of ultra-high performance concrete–a new processing route for architects and builders. Materials & Design. 100, 102-109.